Evaluation of acute supplementation with the ketone ester (*R*)-3-hydroxybutyl(*R*)-3-hydroxybutyrate (ΔG) in healthy volunteers by cardiac and skeletal muscle ^{31}P magnetic resonance spectroscopy

Donnie Cameron[1,2*], Adrian Soto-Mota[3], David R. Willis[1], Jane Ellis[4], Nathan E.K. Procter[1], Richard Greenwood[5], Neil Saunders[5], Rolf F. Schulte[6], Vassilios S. Vassiliou[1], Damian J. Tyler[3], Albrecht Ingo Schmid[4,7], Christopher T. Rodgers[4,8], Paul N. Malcolm[5], Kieran Clarke[3], Michael P. Frenneaux[1], Ladislav Valkovič[4,9]

1) Norwich Medical School, University of East Anglia, Norwich, UK.
2) C.J. Gorter Center for High-Field MRI, Department of Radiology, Leiden University Medical Center, Leiden, The Netherlands
3) Department of Physiology, Anatomy and Genetics, University of Oxford, Oxford, UK
4) Oxford Centre for Clinical Magnetic Resonance Research, Radcliffe Department of Medicine, Division of Cardiovascular Medicine, University of Oxford, Oxford, UK
5) Radiology Department, Norfolk & Norwich University Hospital, Norwich, UK
6) GE Healthcare, Munich, Germany
7) High Field MR Center, Center for Medical Physics and Biomedical Engineering, Medical University of Vienna, Vienna, Austria
8) Wolfson Brain Imaging Centre, Department of Clinical Neurosciences, University of Cambridge, Cambridge, UK
9) Department of Imaging Methods, Institute of Measurement Science, Slovak Academy of Sciences, Bratislava, Slovak Republic

***Corresponding author contact details:** Donnie Cameron, Bob Champion Research & Education Building, University of East Anglia, Norwich Research Park, Norwich NR4 7UQ, United Kingdom. E-mail: Donnie.Cameron@uea.ac.uk. Telephone: +44 (0)1603 591371

The authors would prefer this article to be formatted in British English

ABSTRACT

In this acute intervention study, we investigated the potential benefit of ketone supplementation in humans by studying cardiac phosphocreatine to adenosine-triphosphate ratios (PCr/ATP) and skeletal muscle PCr recovery using phosphorus magnetic resonance spectroscopy (^{31}P-MRS) before and after ingestion of a ketone ester drink. We recruited 28 healthy individuals: 12 aged 23−70 years for cardiac ^{31}P-MRS, and 16 aged 60−75 years for skeletal muscle ^{31}P-MRS. Baseline and post-intervention resting cardiac and dynamic skeletal muscle ^{31}P-MRS scans were performed in one visit, where 25 g of the ketone monoester, deltaG®, was administered after the baseline scan. Administration was timed so that post-intervention ^{31}P-MRS would take place 30 minutes after ΔG® ingestion. The ΔG® ketone drink was well-tolerated by all participants. In participants who provided blood samples, post-intervention blood glucose, lactate and non-esterified fatty acid concentrations decreased significantly (−28.8%, $p \ll 0.001$; −28.2%, $p=0.02$; and −49.1%, $p \ll 0.001$, respectively), while levels of the ketone body D-beta-hydroxybutyrate significantly increased from mean (standard deviation) 0.7 (0.3) to 4.0 (1.1) mmol/L after 30 minutes ($p \ll 0.001$). There were no significant changes in cardiac PCr/ATP or skeletal muscle metabolic parameters between baseline and post-intervention. Acute ketone supplementation caused mild ketosis in blood, with drops in glucose, lactate, and free fatty acids; however, such changes were not associated with changes in ^{31}P-MRS measures in the heart or in skeletal muscle. Future work may focus on the effect of longer-term ketone supplementation on tissue energetics in groups with compromised mitochondrial function.

KEYWORDS

Ketone monoester, ketone bodies, phosphorus MRS, ^{31}P-MRS, heart, skeletal muscle, 3T, 7T

INTRODUCTION

Cardiac and skeletal muscle function declines with age, impairing quality of life in older individuals in a vicious cycle of decreased physical activity and muscle loss. Reduced myocardial function can promote physical inactivity, leading, in turn, to skeletal muscle dysfunction, and this becomes yet more pronounced in cardiac pathologies such as chronic heart failure. Even in relatively healthy older adults, the progressive loss of skeletal muscle mass and overall diminished strength with ageing can eventually develop into sarcopenia (1), a condition estimated to affect up to 10% of the global population (2). The causes of this phenomenon are multi-factorial: hormonal changes with age, denervation of neuromuscular junctions, increased adiposity of skeletal muscle, and inflammatory infiltration, oxidation, or glycation of actin and myosin filaments may all contribute to the development of sarcopenia (1-5). The emergence of overt mitochondrial dysfunction with ageing is also a distinct feature of cardiac and skeletal muscle dysregulation. Studies in mice have shown that declining skeletal muscle functional capacity with age is correlated with mitochondrial dysfunction, with uncoupled mitochondrial respiration, increased reactive oxygen species generation, and altered glucose homeostasis being more apparent in older animals (6, 7). In older humans, loss of skeletal muscle mitochondrial function is correlated with diminished physical function (8). Uncoupled mitochondrial respiration has also been documented in heart failure, (9) particularly when circulating free-fatty acid concentrations are high.

Ketone monoesters represent a promising substrate for addressing the energetic impairments of pathologies such as heart failure and sarcopenia, offering an exogenous, rapidly available alternative to fatty acids or carbohydrates. The importance of nutrition in ameliorating sarcopenia has been recognised (10), and the therapeutic benefits of ketogenic diets and nutritional ketosis have been examined in the context of this disease (11, 12), but studies in sarcopenia to date have not assessed mitochondrial function. Furthermore, whereas typical dietary interventions take several days to produce useful levels of ketone bodies, similar blood concentrations can now be reached within 30 minutes through ingestion of the ketone monoester, (*R*)-3-hydroxybutyl (*R*)-3-hydroxybutyrate. These exogenous ketones have been shown to improve cardiac metabolic efficiency and endurance in rats (13, 14), as well as the intramuscular energy balance during exercise in humans with a fatty acid oxidation disorder (15), as assessed by phosphorus magnetic resonance spectroscopy (^{31}P-MRS). Indeed, ^{31}P-MRS represents an ideal non-invasive modality for assessing the effects of pharmaceutical interventions on tissue bioenergetics *in vivo*. Primary metabolic parameters assessed by ^{31}P-MRS in muscle tissue—namely, the cardiac phosphocreatine to adenosine triphosphate ratio (PCr/ATP) and the rate of recovery of intra-muscular PCr after exercise—have been linked to mitochondrial health (16, 17). Further, similarly to cardiac PCr/ATP (18), the skeletal muscle PCr recovery rate has also been shown to decline with age, with a marked impairment in pre-frail older adults (19).

In this acute intervention study, we used ^{31}P-MRS to investigate the potential benefit of nutritional ketone supplementation in both younger and older adults by studying changes in cardiac PCr/ATP and skeletal muscle PCr recovery following exercise, before and after ingestion of a ketone ester drink.

METHOD

Study population

For cardiac MRS, 12 healthy adults (6 male and 6 female), mean age (range) = 38 (23−70) years were recruited via advertisements displayed at the University of Oxford and on the John Radcliffe Hospital website. For skeletal muscle MRS, a total of 16 older adults (10 male and 6 female), mean age (range) = 67 (60−75) years were recruited through advertisements posted on public notice boards in the Norfolk community. Participants were asked to fast for 24 hours prior to their visit, in order to increase free-fatty acids in blood, but they were encouraged to drink water. Exclusion criteria included: chronic clinical diseases such as cardiovascular disease, diabetes, renal impairment, neurological disorders, or diseases that may affect motor or cognitive function, except for hypertension and hyperlipidaemia; contraindications for

undergoing magnetic resonance imaging and spectroscopy; and participation in ketogenic diets.

The cardiac protocol was preregistered at the ISRCTN (15716557) and approved by the Medical Sciences Interdivisional Research Ethics Committee of the University of Oxford (R50081/RE001). Skeletal muscle procedures were approved by the East of England − Cambridge Central Research Ethics Committee (18/EE/0111). Written informed consent was obtained in all cases and all study activities complied with the Declaration of Helsinki.

Study design

This study was designed as a single-arm clinical study where baseline and post-intervention ^{31}P-MRS were performed in one visit. Subjects underwent either cardiac MRS or skeletal muscle MRS, but not both. After the baseline scan, each subject drank 25 mL of ketone ester, (*R*)-3-hydroxybutyl (*R*)-3-hydroxybutyrate (deltaG®, TΔS Limited, Thame, UK), timed so that the post-intervention ^{31}P-MRS acquisition would take place 30 minutes after ingestion of deltaG®, when βHB concentrations were near maximal (20).

Blood metabolic changes

Cardiac MRS participants gave their first blood sample immediately prior to drinking the ketone ester and undergoing the second scan. The second blood sample was obtained at the end of the second scan, approximately 40 minutes after participants drank the ketone monoester. Plasma from these blood samples was obtained by centrifugation and analysed for blood glucose, lactate, non-esterified fatty acids, and the ketone body D-beta-hydroxybutyrate using a commercial semi-automated bench-top analyser (ABX Pentra, Montpellier, France).

Muscle strength

Skeletal muscle MRS participants underwent muscle strength testing prior to MR procedures, to determine suitable ankle weights for exercise ^{31}P-MRS. Maximum quadriceps muscle strength was defined as the highest of three consecutive values of torque (Nm) measured by left-leg knee extensor contraction at a knee flexion of 90° using a hand-held dynamometer (Lafayette Manual Muscle Testing System Model-01165, Lafayette Instrument Company, Lafayette, IN, USA). Torque was determined as the force generated during knee extension multiplied by the distance from the centre of the knee to the point where the dynamometer was applied to the tibia.

Phosphorus magnetic resonance spectroscopy

Cardiac MR experiments. Cardiac ^{31}P-MRS scans were performed on a whole body 7 Tesla Magnetom MR scanner (Siemens Healthineers, Erlangen, Germany) following procedures described previously by Ellis et al (21). Subjects were scanned head-first supine. A 10 cm ^{1}H transmit/receive loop coil (Rapid Biomedical, Rimpar, Germany) was used to acquire two-chamber, four-chamber and mid-short-axis spoiled gradient-recalled echo stacks of localiser cine images. The ^{1}H coil was then replaced with a 16-element ^{31}P array coil (Rapid Biomedical) consisting of a single rectangular 28 × 27 cm^2 transmit loop and a 4 × 4 matrix of 16 circular flexible receive loops, each 5.5 cm in diameter. The ^{31}P coil was placed in the same position as the ^{1}H coil, above the interventricular septum. Serial, non-localised inversion-recovery acquisitions were performed for the post-hoc determination of transmit efficiency, using measurements from a central spherical phenylphosphonic acid (PPA) fiducial mounted on the coil housing. Custom MATLAB code was then used to determine the coil position from three orthogonal, single-channel ^{31}P spoiled gradient-recalled echo images, localising five PPA fiducials including the centre fiducial used for B_1 determination. B_0 shimming was performed using a custom algorithm, described by Ellis et al. (21). A short 3D ultra-short echo time chemical shift imaging (CSI) sequence was used for signal localisation, with the following parameters: repetition time = 1 s; field-of-view = 200 × 240 × 200 mm^3; matrix size = 8 × 16 × 8; nominal voxel size = 9.4 mL; flip angle at interventricular septum = approximately 30°; shaped radiofrequency excitation pulse with bandwidth = 2000 Hz; acquisition weighting with 4 averages at k = 0; and whitened singular value decomposition (WSVD) coil combination. The CSI grid was planned on a short-axis view of

the heart, with the in-plane matrix parallel to the chest wall. The CSI matrix was fixed at the point of acquisition, and not shifted in post-processing. In order to minimise skeletal muscle signal contamination, a 25 mm thick, B_1-insensitive train to obliterate signal (BISTRO) saturation band was placed in the anterior chest wall (22), The excitation pulse was centred at +266 Hz relative to PCr to cover metabolites from 2,3-diphosphoglycerate (2,3-DPG) to γ-ATP. Respiratory gating and ECG triggering were not used. The total time per exam, including participant set-up, cardiac imaging, and ^{31}P-MRS, was approximately 30 minutes.

Skeletal muscle MR experiments. All skeletal muscle ^{31}P-MRS was performed on a 3 tesla MR750w MRI scanner (GE Healthcare, Milwaukee, WI, USA) equipped with a 15 cm transmit-receive loop coil tuned to phosphorus (PulseTeq, Surrey, UK). Participants were positioned feet-first and supine with the loop coil fastened over their right vastus lateralis, using hook-and-loop straps, midway between the greater trochanter and lateral femoral epicondyle. Participants were then shifted laterally to place the right thigh close to the magnet's isocentre, and additional hook-and-loop straps were applied to their knees to limit gross displacements during the scan. An inversion-recovery fast-spin-echo localiser was applied to verify that the cluster of three fiducials at the centre of the coil was positioned over the vastus lateralis. Then, after manual first-order B_0 shimming, a non-localised ^{31}P-MRS acquisition was performed with a Bloch-Siegert preparation pulse, provided as part of the MNS Research Pack (GE Healthcare, Munich, Germany), to determine the transmit gain needed to achieve a 90° excitation (23). Exercise MRS was applied using a similar design to that described by Sleigh at al. (24). Briefly, the 12-minute protocol consisted of two bouts, each comprising a 1-minute rest period, a 1-minute exercise period, and a 4-minute post-exercise recovery period. The pulse-acquire ^{31}P-MRS acquisition ran continuously over this 12-minute protocol with the following sequence parameters: 240 dynamics with a repetition time = 3 s, spectral bandwidth = 2250 Hz, 2048 sampled points, a resonance frequency offset of 50 Hz, and block excitation with a flip angle of 90°. The total time per exam, including participant set-up, and skeletal muscle imaging and ^{31}P-MRS, was approximately 40 minutes. Participants were given at least a 30-minute break between baseline and post-intervention exams to minimise any effect of fatigue on post-intervention PCr recovery.

Post-Processing

Cardiac muscle spectra. Cardiac spectra from the midseptal voxel were fitted using the Oxford Spectroscopy Analysis (OXSA) toolbox – a MATLAB implementation of the AMARES fitting algorithm (25). The fitted peaks, and their estimated chemical shifts, were: PCr at 0 ppm, γ-ATP at −2.48 ppm, and 2,3-diphosphoglyceric acid (2,3-DPG) at 5.4 and 6.4 ppm. The reported cardiac PCr/ATP values were calculated using the γ-ATP signal, corrected for blood signal contamination via subtraction of 15% of the total 2,3-DPG signal from the measured γ-ATP amplitudes (26), and corrected for partial saturation using relaxation times from the literature (26). Saturation factors were also adjusted for the actual flip angle in the interventricular septum, which was determined from coil position and transmit efficiency measures using the Biot-Savart law. Cramér-Rao lower bounds (CRLBs) were used to express the uncertainty in metabolite concentrations.

Skeletal muscle spectra. Skeletal muscle data were processed using an in-house software pipeline written in MATLAB (2018a, The Mathworks, Natick, MA, USA) and based on a previously-described routine for processing static ^{31}P spectra (27). Briefly, the pipeline comprised 15 Hz Lorentzian line-broadening, two-times zero-filling, zero- and first-order phase correction, frequency and phase alignment of individual dynamic spectra (28, 29), and averaging of spectra in blocks of three. Each series of 80 spectra was then piped into the AMARES algorithm from jMRUI (version 3.0)[1] (30-32), where residual phase errors were corrected, and all metabolite signals were fitted and their amplitudes and chemical shifts calculated: PCr at 0 ppm, γ-ATP at −2.41 ppm, α-ATP at −7.51 ppm, β-ATP at −16 ppm, phosphodiesters (PDE) at 3 ppm, and inorganic phosphate (Pi) at 5.1 ppm. PCr breakdown

[1] www.jmrui.eu

during exercise was determined, and its recovery after exercise cessation was fitted using a mono-exponential rise to a maximum, as follows:

$$\mathrm{PCr}(t) = \mathrm{PCr}_e - \Delta\mathrm{PCr} \cdot \exp^{-t/\tau_{\mathrm{PCr}}}, \quad (1)$$

where PCr_e is the post-recovery PCr signal, ΔPCr is the difference between the post-recovery and end-of-exercise PCr signals, and τ_{PCr} is the time constant of PCr resynthesis. Cytosolic pH was also estimated for each time-point of the dynamic ^{31}P series using the Henderson-Hasselbalch equation:

$$\mathrm{pH} = 6.75 + \log\left(\frac{\delta - 3.27}{5.63 - \delta}\right), \quad (2)$$

where δ is the chemical shift between Pi and PCr. Acidosis was deemed to have occurred if the pH during exercise dropped by more than 0.2 units from the baseline value.(33)

Further exercise MRS measures were calculated using the parameters derived above, including the initial PCr recovery rate:

$$\mathrm{V}_{\mathrm{PCr}} = \Delta\mathrm{PCr}/\tau_{\mathrm{PCr}}\ ; \quad (3)$$

the free adenosine diphosphate concentration:

$$[\mathrm{ADP}] = \left\{\left([\mathrm{TCr}]/[\mathrm{PCr}]\right) - 1\right\} \cdot [\mathrm{ATP}]/\left(K\left[\mathrm{H}^+\right]\right), \quad (4)$$

where the equilibrium constant $K = 1.66 \times 10^9$ L/mol, $[H^+] = 10^{-pH}$, and [ATP] and total creatine [TCr] = 8.2 and 42.5 mmol/L cellular water, respectively (34); and the maximal rate of oxidative ATP synthesis:

$$\mathrm{Q}_{\mathrm{max}} = \left(\mathrm{V}_{\mathrm{PCr}} + \mathrm{Q}_{\mathrm{B}}\right)\left\{1 + \left(\mathrm{K}_{\mathrm{m}}/[\mathrm{ADP}]_{\mathrm{end\_exercise}}\right)^n\right\}, \quad (5)$$

where K_m is the [ADP] at the half-maximal oxidation rate, assumed to be 30 μM (35), Q_b is the basal rate of ATP turnover, estimated at 0.04 mM/s (36), and *n* is the Hill coefficient.

Rest spectra were generated by averaging data from the initial one-minute rest period prior to exercise, for both baseline and post-intervention scans. Fitted peak intensities were relaxation-corrected using T_1 values reported by Bogner et al. (37), and metabolite concentrations were quantified, again assuming an ATP concentration of 8.2 mM/L cellular water (34). Further, ratios of Pi to PCr and PCr to total phosphate were also calculated, where the latter represents the total area under all defined resonances in the spectrum: namely, Pi, PDE, PCr, and the three ATP resonances.

Sample size

Our preliminary work led to the hypothesis that ingestion of 25 g of the ketone ester (*R*)-3-hydroxybutyl (*R*)-3-hydroxybutyrate would lead to an increase of 22% and 15% in the primary outcome measures, cardiac PCr/ATP and skeletal muscle τ_{PCr}, respectively. For cardiac experiments, the variance of PCr/ATP at 7 tesla was assumed to be 22%, based on work by Ellis at al. (21). Thus, for a Type I error rate, α = 0.05, and a Type II error rate, β = 0.2—namely, 80% power— a sample size of n = 12 was required to reject the null hypothesis. Based on the results of Sleigh et al. (24), whose work formed the basis of our exercise ^{31}P-MRS protocol, a variance of 10% or less was assumed for skeletal muscle τ_{PCr}. Selecting a Type I error rate, α = 0.05, and a Type II error rate, β = 0.05—namely, 95% power—a sample size of *n* = 12 would be sufficient to reject the null hypothesis. To allow for drop-outs and technical issues, this recruitment target was increased to *n* = 16. Sample sizes were calculated using G*Power software (version 3.1, Heinrich-Heine-Universität Düsseldorf, Düsseldorf, Germany).

Statistical analysis

All statistical analyses were performed in R (Version 3, R Foundation for Statistical Computing, Vienna, Austria) and Microsoft Excel (Microsoft, Redmond, WA, USA). Data were tested for normality using the Shapiro-Wilk test. Differences between groups were assessed using two-sided Student's *t*-tests when data were normally distributed and Mann-Whitney *U* tests when they were not, and correlations with age were explored using Pearson's *r*. A *p*-value less than 0.05 was considered statistically significant in all analyses.

RESULTS

For cardiac experiments, a total of 12 participants were enrolled, with no exclusions. Of the 16 participants recruited for skeletal muscle MRS, the ^{31}P-MRS datasets of four were excluded due to hardware failure and a further two were discarded due to insufficient PCr breakdown. Participant demographics, after exclusions, are shown in Table 1. Ingestion of the deltaG® ketone drink was well-tolerated by all participants. There were no reports of nausea or lower intestinal complaints, such as intestinal cramps or diarrhoea. Figure 1 shows representative data from the cardiac and skeletal muscle examinations.

Blood metabolic changes

In the subset of participants who provided blood samples (n = 12), post-intervention blood glucose, lactate, and non-esterified fatty acid concentrations were significantly lower than pre-intervention values: mean (SD) = 5.00 (1.01) vs 3.56 (0.66) mmol/L, $p \ll 0.001$; 1.84 (0.45) vs 1.32 (0.32), p = 0.02; and 1.08 (0.32) vs 0.55 (0.20) mmol/L, $p \ll 0.001$, respectively, Blood levels of the ketone body D-beta-hydroxybutyrate were significantly higher after the intervention: mean (SD) = 0.73 (0.32) vs 3.98 (1.07) mmol/L, $p \ll 0.001$. These changes are represented graphically by line plots shown in Figure 2 (top row).

Cardiac muscle experiments

Cardiac ^{31}P-MRS results are listed in Table 2 and shown graphically in Figure 2 (bottom row). CRLBs for all spectra were less than 15% on average. There was no statistically-significant difference in cardiac PCr/ATP post-intervention relative to the pre-intervention value.

Cardiac phosphorus MRS parameters versus age. Relationships between cardiac PCr/ATP and age were explored using Pearson's *r*. There was no correlation between PCr/ATP and age at baseline (r = −0.43, p = 0.16) and neither was there a correlation between change in PCr/ATP and age (r = 0.21, p = 0.52).

Skeletal muscle experiments

All ^{31}P-MRS-derived parameters for skeletal muscle are shown in Table 2, and pre- and post-intervention tau PCr and [PCr] are illustrated in line plots in Figure 2 (bottom row). There were no statistically significant differences in the means of any ^{31}P-MRS parameters post-intervention relative to pre-intervention. No datasets appeared to show acidosis, either pre- or post-intervention.

Skeletal muscle phosphorus MRS parameters versus age. There were no statistically-significant correlations between baseline tau PCr and age or change in tau PCr and age shown by Pearson's r (r = 0.03, p = 0.93; and r = 0.47, p = 0.17, respectively). There were also no correlations observed between: baseline [PCr] and age or change in [PCr] and age (r = −0.31, p = 0.38; and r = −0.18, p = 0.62, respectively); baseline V_{PCr} or change in V_{PCr} and age (r = −0.10, p = 0.79; and r = −0.34, p = 0.33); or baseline Q_{max} or change in Q_{max} and age (r = 0.41, p = 0.28; and r = −0.36, p = 0.34).

DISCUSSION

In this study we conducted an acute intervention of a single ketone ester drink in a cohort of healthy adults, where cardiac and skeletal muscle high-energy phosphate metabolism was monitored via ^{31}P-MRS immediately before, and 30 minutes after, ketone administration. Post-intervention we saw significantly increased blood concentrations of the ketone body **D**-beta-hydroxybutyrate, and a significant decrease in concentrations of glucose, lactate, and non-esterified fatty acids. However, we did not observe any statistically-significant post-intervention changes in cardiac PCr/ATP ratios, or in skeletal muscle PCr recovery rates or metabolite ratios.

One of the primary strengths of this study was the use of ^{31}P-MRS, which is a sensitive and widely-used method for assessing cardiac and skeletal muscle energetics. We used established protocols for both cardiac and skeletal muscle ^{31}P-MRS, taking particular care with regards to repeatability aspects. For cardiac ^{31}P-MRS, we elected to avoid cardiac triggering and respiratory gating to maintain consistent repetition times and avoid unpredictable extensions to scan time. Our assessment of cardiac PCr/ATP was done based on the mid-septal voxel signal, which has been shown to give the most reproducible results (21). For the skeletal muscle ^{31}P-MRS protocol, we averaged the results of two exercise bouts together to improve the precision of our exercise MRS measures, in line with the findings of Sleigh et al. (24). Thus, taking these considerations into account, it is unlikely that the absence of significant differences in ^{31}P-MRS parameters pre- and post-intervention was due to a lack of measurement power (21).

The results we show here may indicate that the previously observed haemodynamic benefits of ketone supplementation (14, 38) are not necessarily caused by an increased availability of ATP, but rather by improved efficiency of its utilisation. Veech has theorised that ketone bodies have a more electronegative character than other metabolites, having more hydrogen atoms per carbon (39). This could allow them to produce a larger proton gradient and, therefore, more efficient utilisation of ATP. This hypothesis could potentially be investigated *in vivo* using saturation transfer experiments at rest and during exercise, which can assess changes in Pi-to-ATP exchange rates due to increased workload (40, 41). Further exercise ^{31}P-MRS analyses could also be performed to calculate the ΔG of ATP hydrolysis (42). Regardless, the fact that we show no post-intervention differences in ^{31}P-MRS measures should not be interpreted as indicating a lack of potential benefits of long-term supplementation, or a lack of efficacy, because our participants were healthy volunteers and supplementation in heart failure patients has already proven to be beneficial (38). These considerations are also supported by a 1.5 tesla ^{31}P-MRS study by Bleeker et al., who showed an increase in skeletal muscle Pi/PCr in patients deficient in very-long-chain acyl-CoA dehydrogenase after acute ketone supplementation (15), and a similar result was also seen in canine myocardium in an earlier study by Kim et al (43). As in this work, Bleeker and colleagues did not show changes in post-exercise PCr recovery after the ketone intervention. In contrast to the study design of Bleeker et al., participants in our study, were asked to fast for 24 hours prior to their visit to maximise blood levels of D-beta-hydroxybutyrate by reducing competition from other energy substrates in meals (20). In terms of the timing of our ^{31}P-MRS procedures relative to ingestion of the deltaG® drink, both we and Bleeker et al. administered the intervention 30 minutes prior to the scan (15). This timing was based on work by Stubbs et al. (20), who showed that blood levels of D-beta-hydroxybutyrate reach a maximum between 30 and 60 minutes after administration—an interval that coincides with the data acquisition in our study. Previous work by Nielsen et al. (38) used a three-hour infusion of βHB salt as their intervention; however, this is not directly comparable to the approach we show here, as our deltaG® drink is a food and, therefore, cannot be infused.

Based on previous data, we anticipated increases in the primary cardiac and skeletal muscle outcome measures, PCr/ATP and τ_{PCr}, respectively, as a result of our acute ketone ester intervention. The rationale for this was based on the fact that fatty acids are the natural ligand of peroxisome proliferator-activated receptor alpha (PPARα), which upregulates the

transcription of uncoupling protein 3 (UCP3), which, in turn, uncouples the mitochondrial membrane and reduces ATP production in the myocardium (44). Notably PCr/ATP correlates with free-fatty acid blood concentration (45), and plasma free-fatty acid concentrations correlate with uncoupling protein expression in the myocardium (46). Given the electronegative advantage of ketone bodies (39), we hypothesised that acute ketosis could improve free-fatty-acid-induced uncoupling and increase ATP concentrations, which could be detected with ^{31}P-MRS. However, we were unable to show the expected positive results in ^{31}P-MRS measures, despite the ketosis in blood in the studied participants. Since our study was powered to detect the anticipated positive effects – a 22% increase in cardiac PCr/ATP and a 15% increase in skeletal muscle τ_{PCr} – we cannot rule out much smaller positive, or negative, effects. Our findings should serve as guidance in terms of possible effect sizes, while our study design and methodology will form a useful template for future investigations. Indeed, it is also worth noting here that the synthetic ketone ester we used was well-tolerated in the acute setting, in line with findings from a recent safety study on long-term ketone supplementation (47), which support longer-term supplementation in future studies, which could also be monitored via ^{31}P-MRS.

There are some limitations to the work reported here. We calculated metabolite concentrations in skeletal muscle based on an assumed ATP concentration of 8.2 mM, whereas ATP concentrations possibly decrease with age. However, we expect this change to be relatively consistent in our group of older participants, and intra-individual comparisons, pre- versus post-intervention are not affected. Indeed, our theory that ketone supplementation leads to increased efficiency of ATP utilisation, and not increased ATP availability, lends itself to this assumption. Another possible limitation is that participants were not selected based on their level of physical fitness. Deconditioned individuals are expected to benefit more from ketone supplementation due to energetic deficits, manifesting as longer PCr recovery time constants and lower cardiac and skeletal muscle PCr/ATPs. Future studies could target older participants who demonstrate some of the hallmarks of frailty, as assessed by grip strength, walking speed, and physical performance batteries.

In conclusion, acute supplementation with a ketone ester drink in healthy volunteers caused mild ketosis in blood, with a concomitant drop in glucose, lactate, and free fatty acids; however, we were not able to detect an effect on ultra-high-field ^{31}P-MRS measures in the heart, or in high-field MRS in resting and exercising skeletal muscle. Future work should focus on the effect of longer-term ketone supplementation on cardiac and muscle energetics, particularly in groups with compromised mitochondrial function.

ACKNOWLEDGEMENTS

This study was funded by a combination of seed funding awarded to D.C. by Norwich Medical School, University of East Anglia, and funding from TdeltaS., Ltd. L.V is a Sir Henry Dale Fellow supported jointly by the Wellcome Trust and the Royal Academy (#221805/Z/20/Z), and he also acknowledges the support of the Slovak Grant Agencies VEGA (#2/0003/20) and APVV (#19-0032). A.I.S. was supported by The Austrian Science Fund (FWF) Schrödinger Fellowship (J 4043). C.T.R. is funded by a Sir Henry Dale Fellowship from the Wellcome Trust and the Royal Society (#098436/Z/12/B) and acknowledges support from the NIHR Cambridge Biomedical Research Centre (BRC-1215-20014). The views expressed are those of the author(s) and not necessarily those of the NIHR or the Department of Health and Social Care. J.E. was funded by the Medical Research Council.

CONFLICT OF INTEREST

Doctor Rolf Schulte is employed by GE Healthcare. The intellectual property covering the uses of ketones and ketone esters is owned by the University of Oxford, the National Institutes of Health, and TΔS Ltd. Should royalties ever accrue from these patents, Professor Kieran Clarke, as an inventor, will receive a share of the royalties under the terms proscribed by the University of Oxford. Professor Kieran Clarke is a director of TΔS Ltd., a company spun out of the University of Oxford to develop and commercialise products based on the science of

ketone bodies in human nutrition. The remaining authors declare that the research was conducted in the absence of any commercial or financial relationships that could be construed as a potential conflict of interest.

AUTHORS' CONTRIBUTIONS

Study conception and design: D.C., A.S.M., N.E.K.P., A.I.S., M.P.F., K.C. and L.V. Acquisition of data: D.C., A.S.M., D.R.W., J.E., R.G., and N.S. Analysis and interpretation of data: D.C., A.S.M., J.E., and C.T.R. Drafting of manuscript: D.C., A.S.M., J.E., N.E.K.P., K.C. and L.V. Critical revision: All authors.

REFERENCES

1. Cruz-Jentoft AJ, Baeyens JP, Bauer JM, Boirie Y, Cederholm T, Landi F, et al. Sarcopenia: European consensus on definition and diagnosis: Report of the European Working Group on Sarcopenia in Older People. *Age and Ageing* (2010) 39(4):412-23. doi: 10.1093/ageing/afq034.

2. Shafiee G, Keshtkar A, Soltani A, Ahadi Z, Larijani B, Heshmat R. Prevalence of sarcopenia in the world: a systematic review and meta- analysis of general population studies. *Journal of Diabetes and Metabolic Disorders* (2017) 16:21. doi: 10.1186/s40200-017-0302-x.

3. Degens H. Age-related skeletal muscle dysfunction: causes and mechanisms. *Journal of Musculoskeletal & Neuronal Interactions* (2007) 7(3):246-52.

4. Walston JD. Sarcopenia in older adults. *Current Opinion in Rheumatology* (2012) 24(6):623-7. doi: 10.1097/BOR.0b013e328358d59b.

5. Marty E, Liu Y, Samuel A, Or O, Lane J. A review of sarcopenia: Enhancing awareness of an increasingly prevalent disease. *Bone* (2017) 105:276-86. doi: 10.1016/j.bone.2017.09.008.

6. Jang YC, Lustgarten MS, Liu Y, Muller FL, Bhattacharya A, Liang H, et al. Increased superoxide in vivo accelerates age-associated muscle atrophy through mitochondrial dysfunction and neuromuscular junction degeneration. *Federation of American Societies for Experimental Biology Journal* (2010) 24(5):1376-90. doi: 10.1096/fj.09-146308.

7. Lee HY, Choi CS, Birkenfeld AL, Alves TC, Jornayvaz FR, Jurczak MJ, et al. Targeted expression of catalase to mitochondria prevents age-associated reductions in mitochondrial function and insulin resistance. *Cell Metabolism* (2010) 12(6):668-74. doi: 10.1016/j.cmet.2010.11.004.

8. Joseph AM, Adhihetty PJ, Buford TW, Wohlgemuth SE, Lees HA, Nguyen LM, et al. The impact of aging on mitochondrial function and biogenesis pathways in skeletal muscle of sedentary high- and low-functioning elderly individuals. *Aging Cell* (2012) 11(5):801-9. doi: 10.1111/j.1474-9726.2012.00844.x.

9. Neubauer S. The Failing Heart — An Engine Out of Fuel. *New England Journal of Medicine* (2007) 356(11):1140-51. doi: 10.1056/NEJMra063052.

10. Welch AA, Hayhoe RPG, Cameron D. The relationships between sarcopenic skeletal muscle loss during ageing and macronutrient metabolism, obesity and onset of diabetes. *Proceedings of the Nutrition Society* (2019) 79(1):158-69. doi: 10.1017/S0029665119001150.

11. Sammarco R, Marra M, Di Guglielmo ML, Naccarato M, Contaldo F, Poggiogalle E, et al. Evaluation of Hypocaloric Diet With Protein Supplementation in Middle-Aged Sarcopenic Obese Women: A Pilot Study. *Obesity Facts* (2017) 10(3):160-7. doi: 10.1159/000468153.

12. Merra G, Miranda R, Barrucco S, Gualtieri P, Mazza M, Moriconi E, et al. Very-low-calorie ketogenic diet with aminoacid supplement versus very low restricted-calorie diet for preserving muscle mass during weight loss: a pilot double-blind study. *European Review for Medical and Pharmacological Sciences* (2016) 20(12):2613-21.

458 13. Murray AJ, Knight NS, Cole MA, Cochlin LE, Carter E, Tchabanenko K, et al. Novel
459 ketone diet enhances physical and cognitive performance. *Federation of American Societies*
460 *for Experimental Biology Journal* (2016) 30(12):4021-32. doi: 10.1096/fj.201600773R.

461 14. Sato K, Kashiwaya Y, Keon CA, Tsuchiya N, King MT, Radda GK, et al. Insulin,
462 ketone bodies, and mitochondrial energy transduction. *Federation of American Societies for*
463 *Experimental Biology Journal* (1995) 9(8):651-8. doi: 10.1096/fasebj.9.8.7768357.

464 15. Bleeker JC, Visser G, Clarke K, Ferdinandusse S, de Haan FH, Houtkooper RH, et
465 al. Nutritional ketosis improves exercise metabolism in patients with very long-chain acyl-
466 CoA dehydrogenase deficiency. *Journal of Inherited Metabolic Disease* (2020) 43(4):787-99.
467 doi: 10.1002/jimd.12217.

468 16. Zane AC, Reiter DA, Shardell M, Cameron D, Simonsick EM, Fishbein KW, et al.
469 Muscle strength mediates the relationship between mitochondrial energetics and walking
470 performance. *Aging Cell* (2017) 16(3):461-8. doi: 10.1111/acel.12568.

471 17. Fabbri E, Chia CW, Spencer RG, Fishbein KW, Reiter DA, Cameron D, et al. Insulin
472 Resistance Is Associated With Reduced Mitochondrial Oxidative Capacity Measured by 31P-
473 Magnetic Resonance Spectroscopy in Participants Without Diabetes From the Baltimore
474 Longitudinal Study of Aging. *Diabetes* (2017) 66(1):170-6. doi: 10.2337/db16-0754.

475 18. Esterhammer R, Klug G, Wolf C, Mayr A, Reinstadler S, Feistritzer HJ, et al. Cardiac
476 high-energy phosphate metabolism alters with age as studied in 196 healthy males with the
477 help of 31-phosphorus 2-dimensional chemical shift imaging. *PLOS ONE* (2014)
478 9(6):e97368. doi: 10.1371/journal.pone.0097368.

479 19. Andreux PA, van Diemen MPJ, Heezen MR, Auwerx J, Rinsch C, Groeneveld GJ, et
480 al. Mitochondrial function is impaired in the skeletal muscle of pre-frail elderly. *Scientific*
481 *Reports* (2018) 8(1):8548. Corrected in: Sci Rep. 2019 Nov 25;9(1):17821.

482 20. Stubbs BJ, Cox PJ, Evans RD, Santer P, Miller JJ, Faull OK, et al. On the
483 Metabolism of Exogenous Ketones in Humans. *Frontiers in Physiology* (2017) 8:848. doi:
484 10.3389/fphys.2017.00848.

485 21. Ellis J, Valkovič L, Purvis LAB, Clarke WT, Rodgers CT. Reproducibility of human
486 cardiac phosphorus MRS (31P-MRS) at 7 T. *NMR in Biomedicine* (2019) 32(6):e4095. doi:
487 10.1002/nbm.4095.

488 22. Luo Y, de Graaf RA, DelaBarre L, Tannús A, Garwood M. BISTRO: An outer-volume
489 suppression method that tolerates RF field inhomogeneity. *Magnetic Resonance in Medicine*
490 (2001) 45(6):1095-102. doi: 10.1002/mrm.1144.

491 23. Schulte RF, Sacolick L, Deppe MH, Janich MA, Schwaiger M, Wild JM, et al.
492 Transmit gain calibration for nonproton MR using the Bloch–Siegert shift. *NMR in*
493 *Biomedicine* (2011) 24(9):1068-72. doi: 10.1002/nbm.1657.

494 24. Sleigh A, Lupson V, Thankamony A, Dunger DB, Savage DB, Carpenter TA, et al.
495 Simple and effective exercise design for assessing in vivo mitochondrial function in clinical
496 applications using 31P magnetic resonance spectroscopy. *Scientific Reports* (2016)
497 6(1):19057. doi: 10.1038/srep19057.

498 25. Purvis LAB, Clarke WT, Biasiolli L, Valkovič L, Robson MD, Rodgers CT. OXSA: An
499 open-source magnetic resonance spectroscopy analysis toolbox in MATLAB. *PLOS ONE*
500 (2017) 12(9):e0185356. doi: 10.1371/journal.pone.0185356.

501 26. Rodgers CT, Clarke WT, Snyder C, Vaughan JT, Neubauer S, Robson MD. Human
502 cardiac 31P magnetic resonance spectroscopy at 7 Tesla. *Magnetic Resonance in Medicine*
503 (2014) 72(2):304-15.

504 27. Cameron D, Welch AA, Adelnia F, Bergeron CM, Reiter DA, Dominguez LJ, et al.
505 Age and Muscle Function Are More Closely Associated With Intracellular Magnesium, as
506 Assessed by 31P Magnetic Resonance Spectroscopy, Than With Serum Magnesium.
507 *Frontiers in Physiology* (2019) 10(1454). doi: 10.3389/fphys.2019.01454.

508 28. Chen L, Weng Z, Goh L, Garland M. An efficient algorithm for automatic phase
509 correction of NMR spectra based on entropy minimization. *Journal of Magnetic Resonance*
510 (2002) 158(1):164-8. doi: 10.1016/S1090-7807(02)00069-1.

511 29. Wiegers EC, Philips BWJ, Heerschap A, van der Graaf M. Automatic frequency and
512 phase alignment of in vivo J-difference-edited MR spectra by frequency domain correlation.
513 *Magnetic Resonance Materials in Physics, Biology and Medicine* (2017) 30(6):537-44. doi:
514 10.1007/s10334-017-0627-y.

515 30. Vanhamme L, van den Boogaart A, Van Huffel S. Improved method for accurate and
516 efficient quantification of MRS data with use of prior knowledge. *Journal of Magnetic*
517 *Resonance* (1997) 129(1):35-43.

518 31. Naressi A, Couturier C, Devos J, Janssen M, Mangeat C, De Beer R, et al. Java-
519 based graphical user interface for the MRUI quantitation package. *Magnetic Resonance*
520 *Materials in Physics, Biology and Medicine* (2001) 12(2-3):141.

521 32. Stefan D, Di Cesare F, Andrasescu A, Popa E, Lazariev A, Vescovo E, et al.
522 Quantitation of magnetic resonance spectroscopy signals: the jMRUI software package.
523 *Measurement Science and Technology* (2009) 20(10):104035.

524 33. Meyerspeer M, Boesch C, Cameron D, Dezortová M, Forbes SC, Heerschap A, et al.
525 (31) P magnetic resonance spectroscopy in skeletal muscle: Experts' consensus
526 recommendations. *NMR in Biomedicine* (2020):e4246. doi: 10.1002/nbm.4246.

527 34. Kemp GJ, Meyerspeer M, Moser E. Absolute quantification of phosphorus metabolite
528 concentrations in human muscle in vivo by 31P MRS: a quantitative review. *NMR in*
529 *Biomedicine* (2007) 20(6):555-65. doi: 10.1002/nbm.1192.

530 35. Kemp GJ, Radda GK. Quantitative interpretation of bioenergetic data from 31P and
531 1H magnetic resonance spectroscopic studies of skeletal muscle: an analytical review.
532 *Magnetic Resonance Quarterly* (1994) 10(1):43-63.

533 36. Jeneson JA, Schmitz JP, van den Broek NM, van Riel NA, Hilbers PA, Nicolay K, et
534 al. Magnitude and control of mitochondrial sensitivity to ADP. *American Journal of*
535 *Physiology-Endocrinology And Metabolism* (2009) 297(3):E774-E84. doi:
536 10.1152/ajpendo.00370.2009.

537 37. Bogner W, Chmelik M, Schmid AI, Moser E, Trattnig S, Gruber S. Assessment of
538 31P relaxation times in the human calf muscle: A comparison between 3 T and 7 T in vivo.
539 *Magnetic Resonance in Medicine* (2009) 62(3):574-82. doi: 10.1002/mrm.22057.

540 38. Nielsen R, Møller N, Gormsen LC, Tolbod LP, Hansson NH, Sorensen J, et al.
541 Cardiovascular Effects of Treatment With the Ketone Body 3-Hydroxybutyrate in Chronic
542 Heart Failure Patients. *Circulation* (2019) 139(18):2129-41. doi:
543 10.1161/CIRCULATIONAHA.118.036459.

544 39. Veech RL. The therapeutic implications of ketone bodies: the effects of ketone
545 bodies in pathological conditions: ketosis, ketogenic diet, redox states, insulin resistance,
546 and mitochondrial metabolism. *Prostaglandins Leukot Essent Fatty Acids* (2004) 70(3):309-
547 19. doi: 10.1016/j.plefa.2003.09.007.

548 40. Sleigh A, Savage DB, Williams GB, Porter D, Carpenter TA, Brindle KM, et al. 31P
549 magnetization transfer measurements of Pi→ATP flux in exercising human muscle. *Journal*
550 *of Applied Physiology* (2016) 120(6):649-56. doi: 10.1152/japplphysiol.00871.2015.

551 41. Tušek Jelenc M, Chmelík M, Bogner W, Krššák M, Trattnig S, Valkovič L. Feasibility
552 and repeatability of localized (31) P-MRS four-angle saturation transfer (FAST) of the human
553 gastrocnemius muscle using a surface coil at 7 T. *NMR in Biomedicine* (2016) 29(1):57-65.
554 doi: 10.1002/nbm.3445.

555 42. Fiedler GB, Schmid AI, Goluch S, Schewzow K, Laistler E, Niess F, et al. Skeletal
556 muscle ATP synthesis and cellular H(+) handling measured by localized (31)P-MRS during
557 exercise and recovery. *Scientific Reports* (2016) 6:32037. doi: 10.1038/srep32037.

558 43. Kim DK, Heineman FW, Balaban RS. Effects of beta-hydroxybutyrate on oxidative
559 metabolism and phosphorylation potential in canine heart in vivo. *American Journal of*
560 *Physiology-Heart and Circulatory Physiology* (1991) 260(6):H1767-H73. doi:
561 10.1152/ajpheart.1991.260.6.H1767.

562 44. Villarroya F, Iglesias R, Giralt M. PPARs in the Control of Uncoupling Proteins Gene
563 Expression. *PPAR Res* (2007) 2007:74364. doi: 10.1155/2007/74364.

564 45. Scheuermann-Freestone M, Madsen PL, Manners D, Blamire AM, Buckingham RE,
565 Styles P, et al. Abnormal cardiac and skeletal muscle energy metabolism in patients with
566 type 2 diabetes. *Circulation* (2003) 107(24):3040-6. doi:
567 10.1161/01.cir.0000072789.89096.10.

568 46. Murray AJ, Anderson RE, Watson GC, Radda GK, Clarke K. Uncoupling proteins in
569 human heart. *Lancet* (2004) 364(9447):1786-8. doi: 10.1016/s0140-6736(04)17402-3.

570 47. Soto-Mota A, Vansant H, Evans RD, Clarke K. Safety and tolerability of sustained
571 exogenous ketosis using ketone monoester drinks for 28 days in healthy adults. *Regulatory*
572 *Toxicology and Pharmacology* (2019) 109:104506. doi: 10.1016/j.yrtph.2019.104506.

573

TABLES

Table 1. Participant characteristics.

	Skeletal muscle cohort	Cardiac cohort
Sex	5 male, 5 female	6 male, 6 female
Age, years	67.3 [60−75]	38.0 [23−70]
Height, cm	171 (13)	175 (9)
Weight, kg	74.1 (12.6)	69.8 (11.7)
BMI, kg/m^2	24.8 (4.2)	22.9 (2.3)
Knee extension strength, N·m	134 (51.6)	–

Data are expressed as mean (standard deviation) or mean [range].

578 ***Table 2. Cardiac and skeletal muscle ^{31}P-MRS parameters, pre- and post-intervention.*** *The* p-
579 *values listed were obtained from two-sided Student's* t*-tests. Data are represented as mean (SD).*
580 *ATP = adenosine triphosphate, PCr = phosphocreatine, PDE = phosphodiesters, Pi = inorganic*
581 *phosphate,* Q_{max} *= maximal rate of oxidative ATP synthesis,* τ_{PCr} *= time constant of PCr resynthesis,*
582 V_{PCr} *= initial rate of PCr resynthesis.*

Cardiac ^{31}P-MRS	Pre-intervention	Post- intervention	Mean difference	*p*-value
PCr/ATP	1.86 (0.30)	1.83 (0.32)	−0.04 (0.42)	0.75
Skeletal muscle ^{31}P-MRS	**Pre-intervention**	**Post- intervention**	**Mean difference**	***p*-value**
Mean τ_{PCr}, s	38.4 (12.2)	38.9 (10)	0.53 (4.63)	0.92
Mean PCr breakdown, %	32.5 (9.10)	34.4 (10.2)	1.90 (3.00)	0.67
V_{PCr} mM/s	0.31 (0.10)	0.33 (0.08)	0.02 (0.05)	0.29
[ADP] end exercise, μM	62.6 (35.2)	57.2 (21.9)	−5.3 (24.9)	0.52
Q_{max}, mM/s	0.57 (0.40)	0.48 (0.40)	−0.09 (0.42)	0.55
Resting [PCr], mM	40.9 (3.26)	42.1 (3.41)	1.18 (2.04)	0.44
Resting [Pi], mM	4.64 (1.18)	4.75 (1.20)	0.11 (1.07)	0.84
Resting [PDE], mM	7.04 (1.40)	7.04 (1.27)	0 (0.88)	0.99
Resting Pi/PCr	0.12 (0.02)	0.13 (0.01)	0 (0.02)	0.59
Resting PCr/Total-phosphate	0.53 (0.02)	0.54 (0.02)	0.01 (0.01)	0.5
Resting pH	7.19 (0.24)	7.21 (0.15)	0.02 (0.13)	0.82

583

584

585

586

587 **FIGURE CAPTIONS**
588

589 **Figure 1**. Representative data from the 7 tesla ^{31}P cardiac magnetic resonance spectroscopy
590 (MRS) acquisition (a and b) and the 3 tesla skeletal muscle acquisition (c, d, e, and f): a) an
591 example of localisation showing a chemical shift imaging grid superimposed on a short-axis,
592 spoiled gradient-recalled echo cine image of the heart, where the red rectangle denotes the voxel
593 of interest and the blue strip represents a saturation band used to suppress signal from skeletal
594 muscle; b) cardiac ^{31}P spectra obtained from the septal voxel shown in a, pre- and post-
595 intervention ('Before' and 'After', respectively); c) an inversion recovery fast spin echo localiser
596 image of a participant's right thigh, showing fiducials at the centre of the 15 cm ^{31}P coil positioned
597 over the vastus lateralis; d) a series of 80 ^{31}P spectra averaged in groups of 3 from the 240 spectra
598 acquired during rest and exercise—exercise spectra are highlighted in red; e) an average rest
599 spectrum obtained during the one-minute rest period at the beginning of the ^{31}P-MRS acquisition;
600 and f) time courses of phosphocreatine (PCr) and inorganic phosphate (Pi) derived from peak
601 fitting of the dynamic spectra from d, with exercise periods indicated in grey. ATP = adenosine
602 triphosphate, a.u. = arbitrary units, 2,3-DPG = 2,3-diphosphoglyceric acid, PCr = phosphocreatine,
603 and PDE = phosphodiesters.
604

605 **Figure 2.** Line plots showing pre- and post-intervention changes in: (top row) blood concentrations
606 of the ketone body D-beta-hydroxybutyrate (βHB), non-esterified fatty acids (NEFA), and glucose;
607 and (middle and bottom rows) ^{31}P magnetic resonance spectroscopy measures of cardiac
608 PCr/ATP; and skeletal muscle tau PCr, PCr/ATP, ADP, initial PCr recovery rate V_{PCr}, and maximal
609 rate of oxidative ATP synthesis Q_{max}. Blue, solid lines indicate participants who showed a negative
610 change in the stated parameter, while red, dashed lines represent a positive change. Black lines
611 show the mean change as well as the standard deviation pre- and post-intervention. ADP =
612 adenosine diphosphate, ATP = adenosine triphosphate, PCr = phosphocreatine.

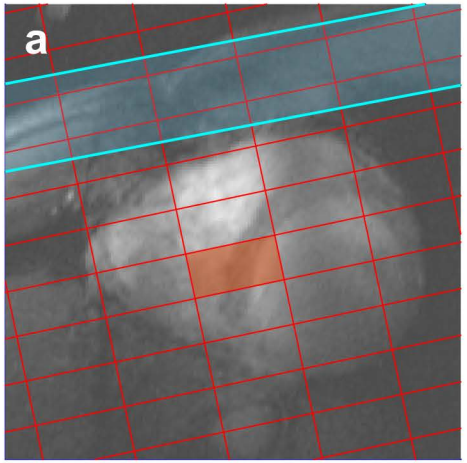
a

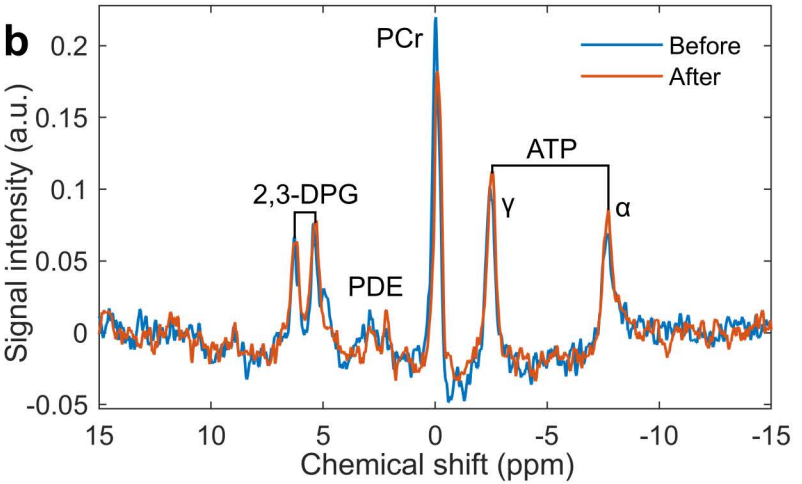
b
PCr
Before
After
ATP
2,3-DPG
γ
α
PDE
Signal intensity (a.u.)
0.2
0.15
0.1
0.05
0
-0.05
15
10
5
0
-5
-10
-15
Chemical shift (ppm)

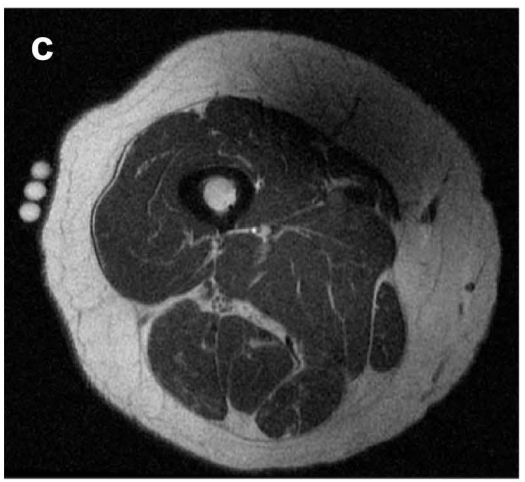
c

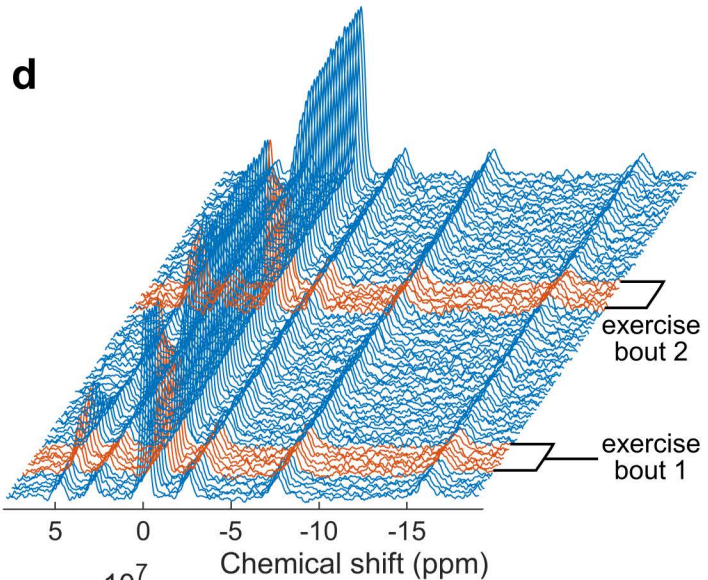
d
exercise
bout 2
exercise
bout 1
5
0
-5
-10
-15
Chemical shift (ppm)

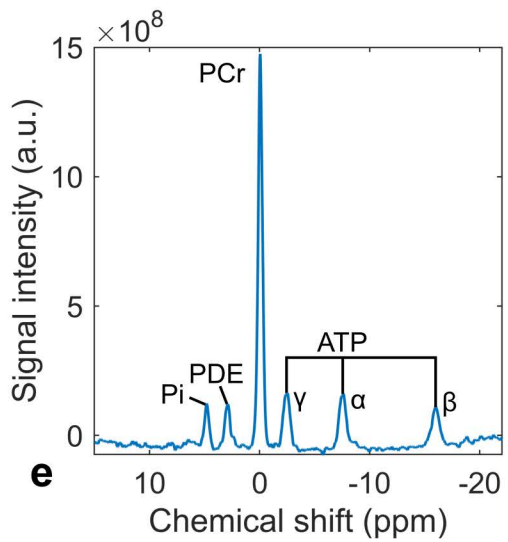
×10^8
15
10
5
0
Signal intensity (a.u.)
PCr
Pi
PDE
ATP
γ
α
β
e
10
0
-10
-20
Chemical shift (ppm)

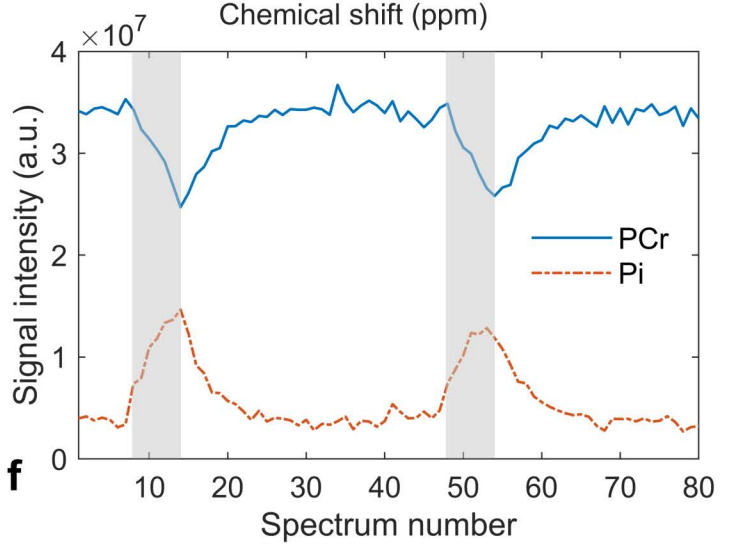
×10^7
4
3
2
1
0
Signal intensity (a.u.)
PCr
Pi
f
10
20
30
40
50
60
70
80
Spectrum number

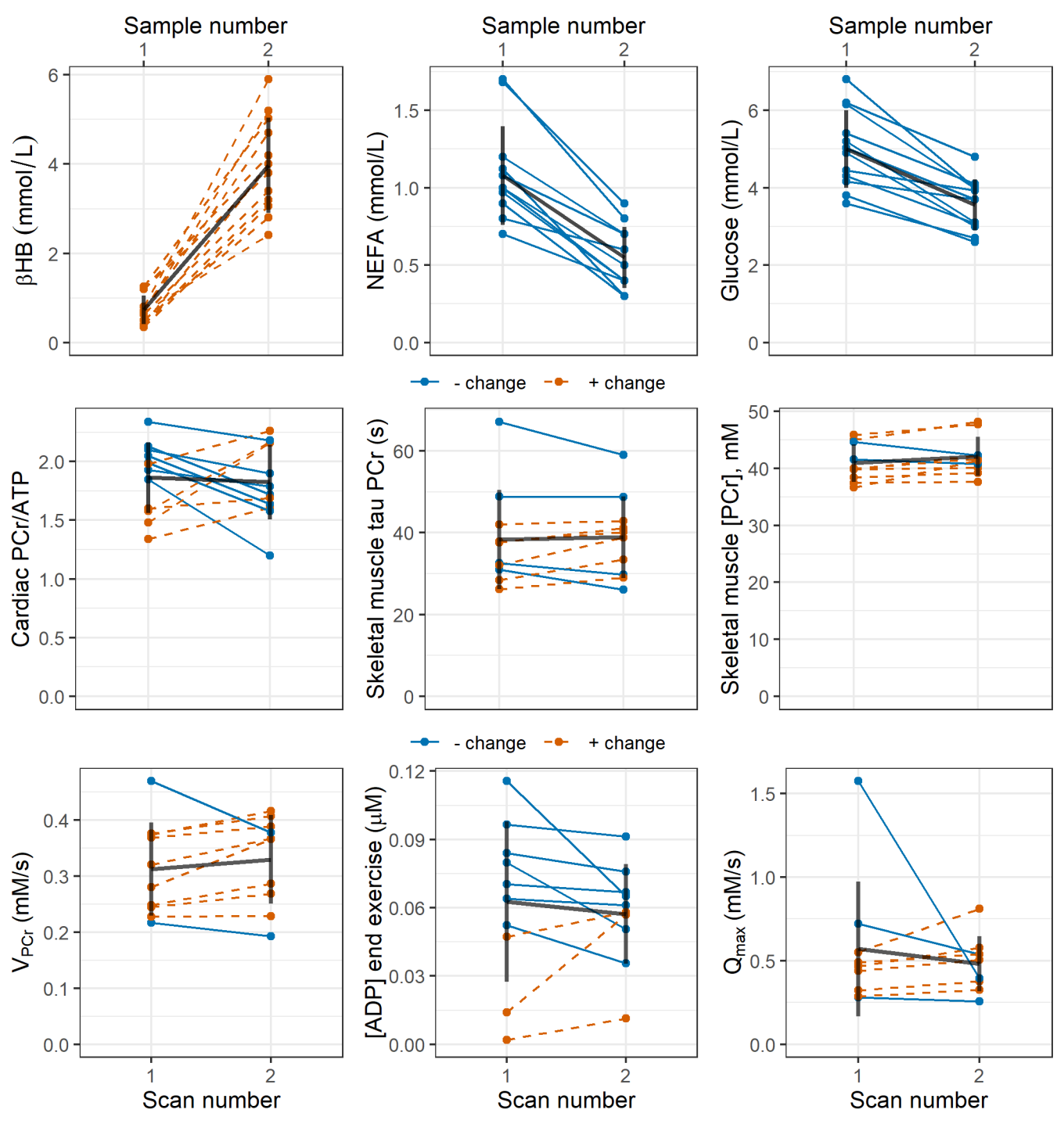
Sample number
1
2
βHB (mmol/L)
0
2
4
6
NEFA (mmol/L)
0.0
0.5
1.0
1.5
Glucose (mmol/L)
0
2
4
6
- change
+ change
Cardiac PCr/ATP
0.0
0.5
1.0
1.5
2.0
Skeletal muscle tau PCr (s)
0
20
40
60
Skeletal muscle [PCr], mM
0
10
20
30
40
50
- change
+ change
V_{PCr} (mM/s)
0.0
0.1
0.2
0.3
0.4
[ADP] end exercise (μM)
0.00
0.03
0.06
0.09
0.12
Q_{max} (mM/s)
0.0
0.5
1.0
1.5
Scan number
1
2